Transport Rate Limited Catalysis on Macroscopic Surfaces: The Activation of Factor X in a Continuous Flow Enzyme Reactor†

Harry A. M. Andree,‡ Paul B. Contino,§ Doris Repke,§ Rodney Gentry,‖ and Yale Nemerson*,‡,§

Department of Biochemistry and Division of Molecular Medicine, Department of Medicine, Mt. Sinai School of Medicine of the City University of New York, 1 Gustave L. Levy Place, New York, New York 10029, and Department of Mathematics and Statistics, University of Guelph, Guelph, Ontario, Canada N1G 2W1

Received October 5, 1993; Revised Manuscript Received December 8, 1993®

ABSTRACT: Blood coagulation is initiated on cells which present a macroscopic surface to the flowing blood stream. We have used a continuous flow enzyme reactor to model this system and to investigate the effects of shear rate and mass transport on the activation of factor X by the complex of the transmembrane protein, tissue factor, and the serine protease, factor VIIa. This initial step of blood coagulation was found to be half-maximal at very low enzyme densities (0.03–0.06%) on the wall of the capillaries. In agreement with hydrodynamic theory, the apparent K_m in the flow reactor was correlated with the cube root of the wall shear rate. These data indicate that at high tissue factor densities (>0.6%) the activation of 150 nM factor X is controlled by the flux of X toward the surface, which is controlled by wall shear rate and substrate concentration. The appearance of the product, Xa, in the effluent was delayed to 8–12 min, which was caused by high-affinity binding of Xa to the phospholipid. This delay was considerably shortened by embedding tissue factor into PC or by coating the PS/PC surface with the phospholipid binding protein, annexin V. At low tissue factor densities, annexin V inhibited X activation by 45%, while no inhibition was observed at high densities. We demonstrate that when the reaction is limited by substrate flux, addition of further enzyme does not increase reaction rates. This contrasts with classical three-dimensional catalysis in which the initial velocity is ordinarily linear with the enzyme concentration.

Enzymatic reactions occurring on macroscopic surfaces have properties quite different from those occurring in solution. One important feature of membrane-bound collisional events was postulated by Berg (1983), who argued from an electrical analogy that half-maximal collisional frequency could be achieved at very low surface coverage by receptors or enzymes. As emphasized by Berg, this phenomenon would allow a cell, with a multiplicity of receptors and enzymes, to exercise many functions in an efficient manner. This important concept has received little attention and to our knowledge no substantial experimental verification.

Examination of Berg's equations indicates that the maximal conversion rate of a catalytic surface can be given by the substrate flux to that surface. The surface density of enzyme molecules required to reach half-maximal efficiency varies with this flux. Thus, at infinitely high substrate flux, half-maximal enzymatic velocity would occur only when the surface was half-occupied by enzyme. Conversely, at very low fluxes, half-maximal velocity would be achieved at very low surface coverage. Put differently, the apparent efficiency of surface-bound enzyme molecules varies with the flux of substrate molecules to the surface.

Investigation of enzyme kinetics on macroscopic surfaces is experimentally difficult. However, two techniques particularly well-suited to this task are ellipsometry (Giesen et al., 1991a,b; Andree et al., 1992) and a continuous flow enzyme reactor (Gemmell et al., 1988, 1990; Repke et al., 1990; Schoen et al., 1990). In each instance substrate molecules are delivered to the surface by a combination of diffusion and convection. Since the flux to the surface has been theoretically described for both instances, both are amenable to quantitative interpretation (Kobayashi & Laidler, 1974; Giesen, 1992). Both techniques have yielded useful data when applied to reactions involved in blood coagulation, a biological system that clearly functions on macroscopic surfaces such as the plasma membranes of various cell types.

In this paper, we investigate the role of substrate transport in determining the enzymatic velocity of a tissue factor-dependent reaction: the activation of factor X by a complex of tissue factor and factor VIIa (TF:VIIa).[1] Tissue factor is a transmembrane protein that is a functional cofactor only when incorporated into phospholipid vesicles or supported bilayers (Nemerson, 1988). Here, we use a previously reported technique to coat the inner surface of glass microcapillary tubes with a single bilayer of phospholipids containing known quantities of tissue factor (Gemmell et al., 1988). The latter is an essential cofactor for factor VIIa, a serine protease of which the precursor exists in human plasma. We perfuse the capillary with saturating quantities of factor VIIa and various concentrations of factor X. Under these conditions the tissue factor remains complexed with factor VIIa, and the system can be treated as if it were a one enzyme–one substrate reaction. By varying the flow rates, and hence the wall shear rates, we

†Supported, in part, by Grant HL-29019 from the National Institutes of Health.

* To whom correspondence should be addressed.
‡ Department of Biochemistry, Mt. Sinai School of Medicine.
§ Division of Molecular Medicine, Mt. Sinai School of Medicine.
‖ University of Guelph.

® Abstract published in *Advance ACS Abstracts,* March 15, 1994.

[1] Abbreviations: TF, tissue factor; VII, factor VII; TF–VIIa, the complex of tissue factor with factor VIIa; X, factor X; Xa, factor Xa; VIIa, factor VIIa; PC, 1,2-dioleoyl-*sn*-glycero-3-phosphatidylcholine; PS, 1,2-dioleoyl-*sn*-glycero-3-phosphatidylserine; IPR-pNA, Ile-Pro-Arg-*p*-nitroaniline; Bis-Tris, bis(2-hydroxyethyl)iminotris(hydroxymethyl)-methane; EDTA, ethylenediaminetetraacetic acid; HEPES, *N*-(2-hydroxyethyl)piperazine-*N*′-(2-ethansulfonic acid); HBS, 0.01 M HEPES, pH 7.5, 0.14 M NaCl, 0.01% NaN_3; HBS-BSA, HBS with 1 mg/mL bovine serum albumin; SD, standard deviation; SE, standard error of the estimate.

0006-2960/94/0433-4368$04.50/0 © 1994 American Chemical Society

are able to vary the transport rate (the substrate flux) of factor X to the surface. We show that the amount of enzyme required to achieve half-maximal conversion of factor X is a function of wall shear rate. Under certain conditions, maximal rates are reached at very low surface coverage by TF:VIIa. Put differently, when the reaction is limited by the transport rate of factor X, many enzyme molecules are silent; i.e., increasing the surface coverage with enzyme does not increase the conversion of factor X to Xa. Thus, at a given concentration of factor X, the dependence of reaction velocity on enzyme density varies with shear rate and can be independent of TF:VIIa. The implication of this phenomenon to physiological coagulation is clear: depending on the caliber of the blood vessel and local flow conditions: changing the enzyme density can either control the reaction velocity or be without substantial effect. Because the activation of factor X by TF:VIIa is also affected by the composition of the phospholipid membrane, we also investigated the effect of the membrane composition on the reaction rates. Finally, we relate our data to observations in the literature regarding "silent" tissue factor molecules on macroscopic surfaces.

MATERIALS AND METHODS

1,2-Dioleoyl-*sn*-glycero-3-phosphatidylserine (PS) and 1,2-dioleoyl-*sn*-glycero-3-phosphatidylcholine (PC) were purchased from Avanti Polar Lipids, Inc. (Alabaster, AL). Human coagulation factor VIIa was purchased from Novo Nordisk A/S 2880 (Denmark), and human factor X was purified as previously described (Miletich et al., 1981). Human annexin V was purified from placenta (Funakoshi et al., 1987). Recombinant human tissue factor (TF) in octyl β-glucopyranoside was a generous gift from Dr. Gordon Vehar, Genentech (South San Fransisco, CA). [^{14}C]PC was purchased from Amersham (Arlington Heights, IL). The chromogenic substrate for factor Xa, Ile-Pro-Arg-*p*-nitroaniline (IPR-pNA), was synthesized in our laboratory. [^{3}H]-TF was prepared by the reaction of TF with succinimidyl [2,3-^{3}H]propionate as per manufacturers instructions (DuPont-NEN Research Products, Boston, MA). Specific activity of [^{3}H]TF was 4.3×10^6 cpm/μg.

Factor Xa Purification. Factor X (3 μM) was activated for 1 h with 1 μg/mL of the X-activating protein from Russel's viper venom (Calbiochem) and 5 mM Ca^{2+}, in HEPES buffered saline (HBS) (0.01 M HEPES, 0.14 M NaCl, 0.01% NaN_3, pH 7.5). Factor Xa was purified on a Mono Q anion exchange column (FPLC, Pharmacia, Piscataway, NJ) using 25 mM Bis-Tris/HCl buffer, pH 6.0, 2 mM EDTA, and a 20-mL gradient from 200 to 350 mM NaCl. Factor Xa eluted at $\approx$310 mM NaCl. Factor Xa was then applied to a Superdex 200 gel filtration column (Pharmacia). This purified factor Xa was used to determine its conversion factor for the chromogenic substrate IPR-pNA and for the binding experiments.

Reconstitution of TF into Phospholipid Vesicles. Tissue factor was reconstituted in vesicles consisting of either 30% PS and 70% PC, or of 100% PC (Bach et al., 1986). Tracers of [^{3}H]TF and [^{14}C]PC were incorporated for quantification of the amounts of TF and phospholipid, respectively. The preparations used typically contained about 200 nM TF and 0.8 mM phospholipid (ratios from 1:3600 to 1:4100).

Changing TF–Phospholipid Ratios. A sample of TF/PS/PC vesicles was mixed with PS/PC vesicles to the desired TF concentration (lipid was maintained at 0.75 mM). This sample was freeze/thawed five times prior to use to assure fully randomized TF orientation (Bach et al., 1986). The ratio of TF to phospholipid was used to calculate the TF density at the wall of the tube. The surface area per phospholipid molecule used for this calculation was 0.65 nm^2 (Kop et al., 1984). To validate this method for changing the TF–lipid ratio, the activity of TF-VIIa was measured in the flow reactor for two preparations: those with a high TF to lipid ratio diluted with additional phospholipid yielded TF-VIIa activities similar to those of preparations with a low TF to lipid ratio (data not shown).

Continuous Flow Reactor Assays. The instrumental setup for the automated flow reactor system is as previously described (Contino et al., 1991). Borosilicate microcapillary tubes (0.27 mm inner diameter $\times$ 128 mm, 1.08-cm^2 surface area, and 7.3-μL volume) were cleaned (Repke et al., 1990) and filled with the appropriate TF–phospholipid mixture at room temperature and incubated for 20 min. Thereafter, the tubes were flushed with HBS-BSA for 8 min at a wall shear rate (γ_w) of 3000 s^{-1}. The coated tubes were then perfused with a reaction mixture containing factors VIIa (10 nM), X (150 nM), and Ca^{2+} (5 mM) in HBS–BSA at γ_w = 1600 s^{-1} at 37 °C. The perfusate from individual tubes was collected at timed intervals into the wells of ELISA plates containing 125–150 μL of 50 mM EDTA and 1 mg/mL BSA, pH 7.5. The Xa concentration was measured after addition of 25 μL of 10 mM of the chromogenic substrate IPR-pNA at 35 °C using a kinetic ELISA plate reader (TMax, Molecular Devices, Menlo Park, CA). The slope of the change in absorbance at 405 nm was taken as the measure of Xa formed. To establish the amount of bound factor Xa, following the perfusion experiment, the capillary was immediately mounted to a pipet with flexible tubing and repeatedly flushed with 10 μL of 50 mM EDTA/BSA into a well of an ELISA plate filled with 90 μL of EDTA. The contents of the well were mixed and diluted into adjacent wells.

Determination of K_d. The K_d of factor Xa for 30% PS/70% PC was measured using the flow reactor. The capillaries were perfused at a γ_w of 1600 s^{-1} for variable lengths of time (50–60 min for factor Xa concentrations above 50 nM and at least 2.5 h for Xa concentrations below 50 nM) with factor Xa to reach equilibrium. Equilibrium conditions were experimentally verified by showing that, at a factor Xa concentration of 10 nM, the lowest concentration used, the binding did not increase if the perfusion time was increased from 1 to 3 h. The capillaries were then washed with EDTA as described above. The amount of factor Xa bound to the wall exceeds the amount of factor Xa free in the tube by a factor of 6 or more. Factor Xa binding was corrected for factor Xa in solution. The binding of factor Xa (Γ, pmol/cm^2) at equilibrium was fit using a unweighted nonlinear least-squares fitting program according to

$$\Gamma = \Gamma_{max}[Xa]/(K_d + [Xa]) \quad (1)$$

with Γ_{max} the maximal binding of factor Xa (pmol/cm^2), [Xa] the free factor Xa concentration (nM), and K_d the dissociation constant (nM).

RESULTS

Hydrodynamic Properties of the Flow Reactor. The average transport rate limit [V, pmol/(min·cm^2)] of a bulk concentration of factor X (S, pmol/mL) to the wall of a capillary with length L (cm) can be calculated from (Kobayashi & Laidler, 1974)

$$V = kS \quad (2)$$

with k (cm/s) the mass transfer coefficient:

$$k = c_0(\gamma_w D^2/L)^{1/3} \quad (3)$$

where

$$\gamma_w = 4Q/(\pi r^3) \quad (4)$$

with D the diffusion coefficient of the protein (cm^2/s), γ_w the wall shear rate (s^{-1}), Q the volumetric flow rate (mL/s), r the internal radius of the capillary (cm), and coefficient $c_0 = 3^{4/3}/[2\Gamma(1/3)] \approx 0.81$, where $\Gamma(1/3)$ is the mathematical Γ function[2] of $^1/_3$, not to be confused with binding in eq 1. For tubes with a radius of 0.0135 cm, the wall shear rates at flow rates of 0.012 and 0.185 mL/min are 100 and 1600 s^{-1}, respectively. Since no value for the diffusion coefficient of factor X is reported in the literature, we used the value of $D_{37} = 9 \times 10^{-7}$ cm^2/s, which is the value of D_{20} of 6.2×10^{-7} cm^2/s for prothrombin, a molecule slightly larger than factor X, adjusted for temperature (Lim et al., 1977; Giesen et al., 1992; Bird et al., 1960). With the given geometry of our tubes, the calculated average mass transport coefficients at γ_w of 100 and 1600 s^{-1} are 1.5 and 3.8×10^{-4} cm/s, respectively. For a substrate concentration of 150 nM and $\gamma_w = 1600$ s^{-1}, this results in a theoretical transport rate to the surface of 3.4 pmol/(min·cm^2). Under conditions where catalysis causes a substrate depletion at the wall, an increasing radial substrate gradient is established from the wall toward the center of the tube. The average thickness of this substrate boundary layer (δ) is given by (Cussler, 1984)

$$\delta = (2/3)(4\pi r^2 DL/Q)^{1/2} \quad (5)$$

The average boundary layers in our system are 20 and 78 μm for shear rates of 1600 and 100 s^{-1}, respectively. At the outlet of the tube, the boundary layer is thus 117 μm thick for γ_w of 100 s^{-1}.

The TF density in the flow reactor can be calculated as follows: For example, a capillary was coated with vesicle preparations consisting of ≈200 nM TF and 0.75 mM phospholipid (ratio 1:3750). As TF is randomly distributed on the inner and outer leaflet of the vesicles (Bach et al., 1986) and the lipid surface density is 0.5 nmol/cm^2, this results in a TF density of 67 fmol/cm^2. Assuming an average radius for TF-VIIa of 3.2 nm (Waxman et al., 1993), this density covers about 1.3% of the surface with TF-VIIa. Similarly, a TF density of 3 fmol/cm^2 (TF to lipid ratio = 1:83000) results in a surface coverage of 0.06%.

Product Formation at the Transport Rate Limit. The effect of TF density on the steady state Xa production by TF-VIIa is presented in Figure 1. The average factor Xa production by 70 fmol of TF-VIIa/cm^2 at γ_w of 1600 s^{-1} for 11 experiments was 2.0 ± 0.2 pmol/(min·cm^2) (mean ± SD), which corresponds to 11.7 ± 1.2 nM at the outlet. This production rate is 60% of the theoretical transport rate as calculated using eqs 2 and 3. The TF density plots were fit to the equation for a hyperbola, thereby defining two parameters, $K_{1/2\,E}$, the density required for half-maximal rates, and $V_{max\,E}$, the velocity predicted when the surface is saturated with enzyme. The results of the fit are shown in Table 1.

The ratio of $V_{max\,E}$ at 1600:100 s^{-1} is 3.0, while based on a transport limited conversion a ratio of $16^{1/3} = 2.5$ would be expected. The Xa production rate was independent of the enzyme density in the range of 35–70 fmol/cm^2. These TF densities are much higher than previously used in our flow reactor system (ratio of 1:100 000 ≈2.5 fmol of TF/cm^2) (Gemmell et al., 1988, 1990; Repke et al., 1990). The $K_{1/2\,E}$ was also dependent on the wall shear rate (Table 1). At 1.7–3.3 fmol of TF/cm^2 only 0.03–0.06% of the surface is covered with enzyme. At $\gamma_w = 1600$ s^{-1}, the activation rate of factor X with 3.3 fmol of TF/cm^2 was 1.07 pmol/(min·cm^2), which is equivalent to 324 conversions per min per enzyme molecule, as compared to 31 conversions per min per enzyme molecule at 70 fmol/cm^2, thus showing the excess catalytic capacity at high TF densities.

In Figure 2, steady-state Xa production was measured as a function of the substrate concentration at wall shear rates of 100 and 1600 s^{-1}. Since the substrate concentrations used are below the K_m(app), the (classical) V_{max} had to be estimated by a different method. With the substrate concentration (150 nM) far above the K_m of 16 nM (Nemerson & Gentry 1986), the k_{cat} can be estimated from the first derivative of the TF density plot (Figure 1) as TF density approaches zero. The k_{cat} ($V_{max\,E}/K_{1/2\,E}$) value was found to be 650 min^{-1}, which

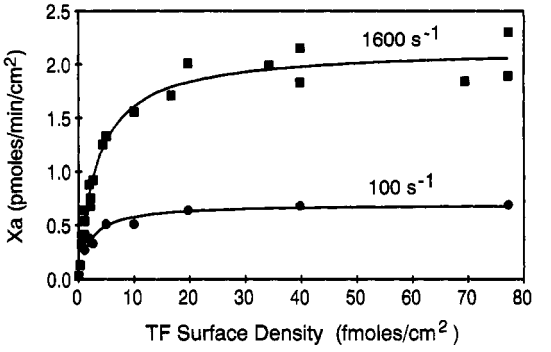

FIGURE 1: Factor X activation in the flow reactor was measured as a function of the TF-density. Capillaries were coated with 0.75 mM PS/PC (30/70) containing various amounts of TF and were perfused with 150 nM X and 10 nM factor VIIa at 37 °C. The X activation rate was measured after steady state was reached. The wall shear rates were 100 (●) and 1600 (■) s^{-1}.

Table 1: Parameters of TF Density Titrations[a]

γ_w (s^{-1})	$K_{1/2\,E}$ (fmol/cm^2)	$V_{max\,E}$ [pmol/(min·cm^2)]
100	1.7 ± 0.4	0.72 ± 0.03
1600	3.3 ± 0.3	2.14 ± 0.06

[a] The TF density plots of Figure 1 were fit to a hyperbola. The maximal Xa production rate when the surface is saturated with enzyme ($V_{max\,E}$) and the TF density that results in half-maximal velocity ($K_{1/2\,E}$) are shown.

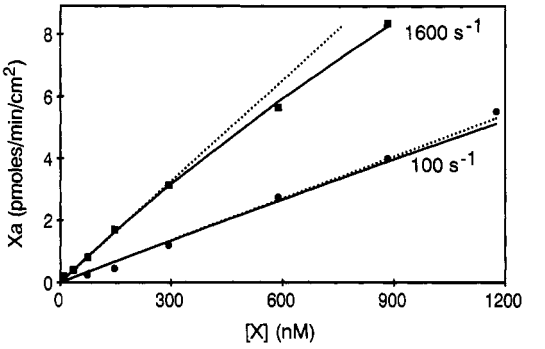

FIGURE 2: Factor X activation was measured as function of substrate concentration for wall shear rates of 100 (●) and 1600 (■) s^{-1}. Glass capillaries were coated with a PS/PC bilayer containing 70 fmoles TF/cm^2 and were perfused with 10 nM factor VIIa and the indicated X concentration. The solid curves show the fits to the Michaelis-Menten equation. The dotted lines represent the first derivatives of these fits.

[2] The Γ function (Hodgman, 1961).

$$\Gamma(a) = \int_0^\infty e^{-x} x^{a-1}\,dx$$

The Γ function is an extension to all real numbers of the factorial function, in the sense that, for an integer n, $\Gamma(n) = (n-1)!$.

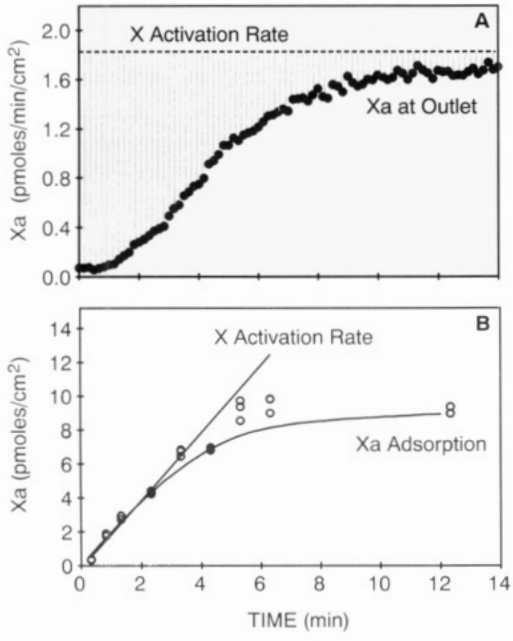

FIGURE 3: (A) Factor Xa production in a capillary coated with 70 fmol of TF/cm² was started by perfusion with 150 nM factor X and 10 nM factor VIIa. The dashed line shows the steady-state Xa production rate, which was reached after 12 min. The shaded area indicates the difference between Xa production measured in the steady state and Xa measured at the outlet. (B) The straight line indicates the cumulative amount of factor Xa produced as calculated from the steady-state production rate. The curved line shows the integral over time of the difference between steady-state factor Xa production (dashed line) and the amount of factor Xa measured at the outlet of the tube (the shaded area in panel A). This deficit represents the amount of factor Xa bound in the tube. The open circles indicate the amount of factor Xa bound to the phospholipid surface, as was determined by rinsing the capillaries with an EDTA solution.

is in agreement with values published earlier (Bach & Rifkin, 1990; Gemmell et al., 1990). The X titration curves in Figure 2 were fit to the Michaelis–Menten equation using this k_{cat} value. The ratio of the fitted K_m(app) values of 10 and 4 μM for γ_w = 100 and 1600 s^{-1}, respectively, is 2.5. We note that this ratio is relatively insensitive to the k_{cat}; e.g., if the k_{cat} were one-half of the fixed value, K_m(app 100)/K_m(app 1600) would be 2.9, while a two times higher k_{cat} would result in a ratio of 2.4.

If the effect of the intrinsic K_m on the initial slope is neglected (Nemerson & Gentry, 1986), the mass transport coefficient is given by V_{max}/K_m(app). The mass transport coefficient of X toward the surface is then 1.9×10^{-4} cm/s at 1600 s^{-1} and 0.7×10^{-4} cm/s at 100 s^{-1}, which is about 50% of the value as calculated with eq 3. The ratio of the initial slopes of 2.5 is in excellent agreement with the value of $(1600/100)^{1/3}$ = 2.5 expected from eq 3, thus suggesting that the Xa production is governed by the transport of X toward the catalytic surface and is not under kinetic control.

The Lag in Factor X_a Appearance. The Xa production profile in a typical flow experiment started by perfusing with 150 nM factor X and 10 nM factor VIIa at a γ_w of 1600 s^{-1} is presented in Figure 3A. The dashed line indicates the steady-state production rate of Xa, which was reached after 12 min, whereas the average passage time of the buffer in the capillary is 0.04 s, which is calculated by dividing the volume of the tube by the volumetric flow rate. This delay in the appearance of factor Xa at the outlet could be caused by a slow assembly of the TF–VIIa complex. This hypothesis was tested by preperfusing the tubes with 10 nM VIIa for 10 min at a γ_w of 1600 s^{-1}; the results (not shown) were similar to the control experiments without the preperfusion, indicating that a slow

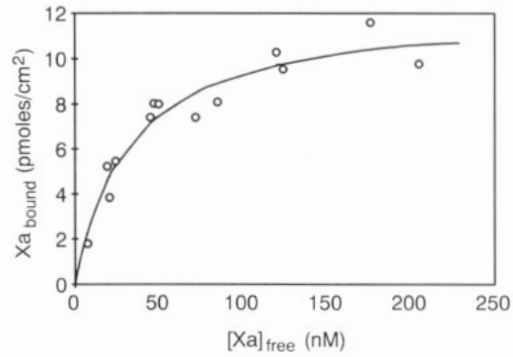

FIGURE 4: Binding isotherm of factor Xa for 30% phosphatidylserine and 70% phosphatidylcholine. Capillaries were coated with a phospholipid mixture which included 70 fmol of TF/cm². They were perfused with the indicated factor Xa concentration. After 0.8–3 h the capillaries were flushed with an EDTA solution to determine the amount of factor Xa bound. A nonlinear least-squares fit indicated a K_d value of 33 ± 6 nM and maximal binding of 12 ± 1 pmol/cm².

assembly of TF-VIIa does not explain the gap in Xa generation. The delay could, however, be caused by binding of factor Xa to the phospholipid bilayer on the wall of the capillaries. To test this hypothesis, the capillaries were removed from the flow reactor and repeatedly washed with 10 μL of 50 mM EDTA. This method allowed the determination of the total amount of factor Xa in the tubes. Because of the large surface area (1.08 cm²) and small volume (7 μL) of the capillaries, the amount of factor Xa in solution was less than 1% of the total amount of factor Xa. Even if all factor X in solution were converted to factor Xa, the amount of factor Xa in solution would be less than 11% of the total amount. Bound Xa, calculated as the difference between total factor Xa and Xa in the solution, is indicated in Figure 3B. If Xa production started immediately, then the deficit in the Xa appearance in the effluent at the outlet should be equal to the amount of factor Xa bound to the wall of the capillary. The integral of the difference between steady-state factor Xa production and factor Xa measured at the outlet of the tube in time (shaded in Figure 3A) corresponds well with the factor Xa adsorption (Figure 3B); accordingly, we can attribute the delay to factor Xa binding.

Determination of K_d for Xa and PS/PC. One of the factors regulating the binding of human factor Xa is its dissociation constant for the phospholipid on the wall. We were able to determine factor Xa bound by perfusing capillaries with factor Xa (Figure 4) and then eluting them with EDTA as above. Equilibrium conditions were experimentally verified by showing that the factor Xa binding at a free concentration of 10 nM did not increase if the perfusion time was increased from 1 to 3 h. Factor Xa concentrations in the perfusate at the end of the experiment were indistinguishable from the Xa concentrations in the starting material. The amount of factor Xa in solution at the highest concentration was only 15% of the amount of factor Xa bound to the phospholipid surface. Figure 4 shows the binding of Xa as a function of the free factor Xa concentration. Nonlinear least-squares fitting resulted in a value for maximal binding of 12 ± 1 pmol/cm² (mean ± SE) and a dissociation constant of 33 ± 6 nM (mean ± SE) of factor Xa for lipid composition of 30% PS and 70% PC employed in these experiments. These values for human factor Xa agree well with literature values determined for binding of bovine factor Xa to 20–25% PS (Nelsestuen & Broderius, 1977; Krishnaswamy et al., 1988; Giesen et al., 1991b). In the activation experiments performed for Figure 3 we observed 8–10 pmol of factor Xa bound to the phospholipid, which is thus close to a monolayer of protein. The concentration of factor Xa close to the wall in Figure 3

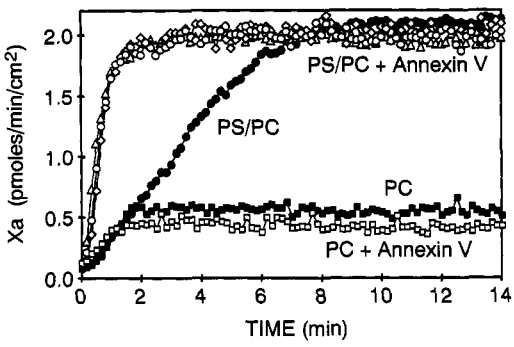

FIGURE 5: Effect of annexin V on the Xa production in the flow reactor. Factor Xa production in the control experiments with 70 fmol of TF/cm² embedded in 30/70 PS/PC (●) or 100% PC (■) was started by perfusion with 150 nM factor X and 10 nM factor VIIa. The annexin V experiments were preperfused with 1 μM annexin V solution in the presence of 5 mM Ca^{2+} for 4 min. Then factor Xa production was measured with 6 (◇), 12 (○), or 24 (△) nM annexin V added to the perfusion buffer. Factor Xa production by TF-VIIa in PC in the presence of 24 nM annexin V is also shown (□).

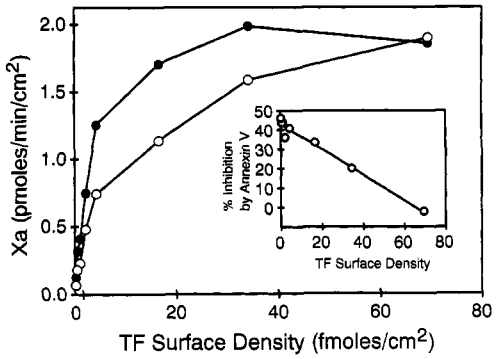

FIGURE 6: Factor Xa production was measured as function of the TF density (●). TF was embedded in 30/70 PS/PC. Annexin V experiments (○) were preperfused with 1 μM annexin V for 4 min, and 24 nM was added to the perfusate. The inset shows the inhibition of TF-VIIa activity by annexin V calculated from paired experiments.

can then be estimated from the binding isotherm (Figure 4) to be between 50 and 150 nM. This is in apparent contrast with the factor Xa concentration measured in the effluent at the outlet of the tube of only 11.7 nM. The difference can be explained by the transport of factor Xa from the surface to the effluent (see Discussion).

Effect of Annexin V on the Appearance of X_a. Annexin V, a protein with a high affinity for phospholipids, is able to compete with other proteins for phospholipid binding (Reutelingsperger et al., 1988; Tait et al., 1989; Andree et al., 1990). The capillaries were preperfused with 1 μM annexin V for 4 min to allow saturation of the phospholipid surface. Then, the reaction was started as described in Figure 3 with annexin V included in the perfusate (Figure 5). A similar steady-state factor Xa production was observed in the presence of 6–24 nM annexin V, 2.0 ± 0.1 pmol/(min·cm²) (mean ± SD, $n = 5$), as was measured for the control experiments. The delay of factor Xa at the outlet of the tube, however, was considerably shortened, and the amount of factor Xa bound to the phospholipid at the end of the experiment was reduced from 8–10 to 3 pmol/cm². The delay in the Xa appearance was reduced to less than 2 min with 70 fmol of TF/cm² embedded in PC. In this case, annexin V had no effect on the delay but caused a small inhibition of the steady-state activation rate. Like for the tubes coated with PS/PC, the amount of factor Xa bound to PC was determined. The total amount of factor Xa found in the tubes coated with PC was 0.58 ± 0.16 (pmol/cm², ± SD). The reduced binding of Xa to PC thus was correlated with the shortened lag observed with this surface.

Effect of Annexin V on Xa Production. The lack of inhibition of TF-VIIa activity by annexin V is seemingly in contrast with other studies (Gramzinski et al., 1989; Ravanat et al., 1992). This might, however, be explained by the high TF surface density used in the present study. The effect of TF density on the inhibition of TF-VIIa activity by annexin V is presented in Figure 6. As described above, the capillaries were preperfused with 1 μM annexin V, and 24 nM annexin V was added to the reaction mixture. The inhibition of TF-VIIa activity by annexin V, shown in Figure 6, is dependent on the TF density and can be linearly extrapolated to be 45% at infinitely dilute enzyme concentrations.

DISCUSSION

The data presented in this paper confirm Berg's prediction that half-maximal reaction rates on two-dimensional surfaces can be achieved with sparse surface coverage with enzyme (Berg, 1983). In Figure 1, we show that the production of factor Xa [pmol/(min·cm²)] approaches a maximum at surface coverages above 0.6% (30 fmol/cm²). We also show, as expected from Berg's treatment, that the amount of enzyme required to reach half-maximal reaction rates varies with substrate flux to the surface. This is evident from the data in Figure 1 in which two wall shear rates were employed with a single substrate concentration. Classical hydrodynamic treatments predict that the substrate flux varies with the cube root of the wall shear rate (Kobayashi & Laidler, 1974). The maximum rate predicted from fitting the data obtained at a wall shear rate of 1600 s^{-1} to a hyperbola is 2.14 pmol/(min·cm²). From this determination, one would then predict a product flux at a wall shear rate of 100 s^{-1} of 0.85 pmol/(min·cm²), and we experimentally determined a maximum flux of 0.72 pmol/(min·cm²), obviously in good agreement with theory.

We also observed that the amount of enzyme required to achieve half-maximal rates was found to be 3.3 and 1.7 fmol/cm² for wall shear rates of 1600 and 100 s^{-1}, respectively. The latter finding indicates that the surface coverage with enzyme required for half-maximal rates varies with the substrate flux to the surface. This conclusion was confirmed in the data presented in Figure 2. Here, we varied the substrate concentration at a constant TF surface density (70 fmol/cm²) at shear rates of 1600 and 100 s^{-1}. The data imply a K_m(app) of 4 and 10 μM, respectively. We note that these values also vary with the cube root of the wall shear rate, as predicted by theory (predicted ratio 2.5, determined ratio 2.5; eqs 2 and 3).

Taken together, these data indicate that the system employed behaves as predicted by hydrodynamic theory. We now argue that the experiments indicated in Figure 1 yield an empirical flux (transport rate) of factor X to the surface: 2.14 and 0.72 pmol/(min·cm²) for the high and low shear rates, respectively. However, these values are lower than those predicted from eqs 2 and 3 and must therefore be rationalized.

First, there are two trivial explanations that could explain these discrepancies, neither of which we believe to be valid. The value we used for the diffusion of factor X could be off by a factor of 2.2 or the estimation of protein concentration could be in error by 70%. Since the value for factor X diffusion is typical for proteins of this size and our measurement of factor X is a simple photometric determination, neither of these possibilities appear reasonable.

Second, the theoretical development for the delivery of substrate to the wall of a tube with convective flow is based on assumptions concerning boundary conditions that are not

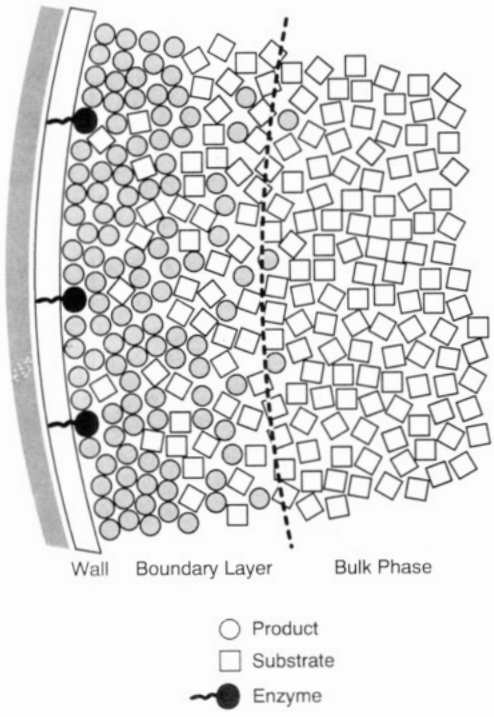

FIGURE 7: Schematic of surface-mediated catalysis. Substrate is transported to the wall of the capillaries and converted to product. A gradient of decreasing substrate concentration is thus formed. Conversely, product formed at the wall is transported from the surface to the bulk. Note that the center of the tube contains little product, and there is no depletion of substrate in the central core.

"well posed" and which must be approximately met to formulate solutions (Bird et al., 1960). The model assumes a tube of sufficient length to enable one to ignore the effect of the portion of the reactor in which the flow profile is established. Moreover, the treatment requires a "short" tube, which means that the boundary layer thickness, δ, is small compared to the tube radius. This assumption essentially means that the concentration in a central core of the tube remains constant and that only substrate molecules in the substrate boundary layer are involved in the reaction (Figure 7). We note that as the length of a tube with a catalytic surface increases, the classical treatment will overestimate the mass transfer to the surface. This becomes intuitively clear if one considers that as the tube length goes to infinity, the average flux to the surface goes to zero. Thus, it is difficult to determine precisely the conditions under which eqs 2 and 3 accurately predict substrate flux. It is clear, however, that as tubes grow longer, the classical theory will overestimate the flux. According to the theory the boundary layer at the outlet of the tube at γ_w of 100 s^{-1} is close to the tube radius. It is therefore the lowest wall shear rate at which substrate depletion may be neglected. Our system would enable one to determine experimentally the tube length that satisfies the boundary conditions assumed in these equations, something we hope to accomplish in the future.

It is important to note that, at the highest enzyme concentrations used (70 fmol/cm^2), the vast majority of the enzyme molecules are unoccupied by substrate and are therefore catalytically silent. The occupation of the enzyme at lower TF densities (3 fmol/cm^2) is about 10 times higher. This conflicts with Michaelis–Menten kinetics, where initial rates are linear with the enzyme concentration. The effect can be modeled by combining local Michaelis–Menten catalysis and substrate transport (Kobayashi & Laidler, 1974). At the transport limit, essentially every molecule of substrate that reaches the surface is converted to product. This is the fundamental reason that increasing the enzyme density does not increase the reaction rates. This phenomenon illustrates the essential difference between two- and three-dimensional catalysis.

Because of the excess catalytic capacity, it follows that the reaction is not kinetically controlled; rather, it is simply controlled by the rate at which substrate is transported to the surface. It is for this reason that we assert that the reaction rate equals the transport rate. Nonetheless, the transport rate of factor X to the surface as calculated using eqs 2 and 3 yields values approximately 1.7-fold higher. We believe that this discrepancy resides in uncertainties in the "classical" hydrodynamic treatment.

The flow reactor experiments are complicated by the potential binding of both factor X and Xa to the lipid surface. This phenomenon bears on the delay in the appearance of Xa in the effluent. We show that this delay is not explained by a slow formation of the TF–VIIa complex: preperfusion of the capillaries with VIIa had no effect on the lag. Rather, our data show that Xa does not reach steady-state levels in the tube effluent until the Xa binding sites on the wall are essentially saturated (Figure 3). We were able to show this using two different techniques. First, we determined the amount of Xa bound to the wall as a function of time. This was then correlated with the appearance of Xa in the effluent; the data (Figure 3) indicate that steady-state levels of Xa in the effluent were not reached until the wall approached saturation. In addition, we used annexin V as a ligand competing for phospholipid binding sites. The addition of annexin V to the reaction essentially eliminated the lag, and the appearance of product in the effluent approached theoretical. The same shortening of the lag was observed with TF–PC, which can be ascribed to the minimal factor Xa binding to PC.

Annexin V, a protein with a high affinity for anionic phospholipid surfaces, has been shown to inhibit phospholipid-dependent blood coagulation reactions by interference with phospholipid binding and impairment of lateral transport (Reutelingsperger et al., 1988; Tait et al., 1989; Thiagarajan et al., 1990; Andree et al., 1992). The lateral transport of substrate to the prothrombinase complex, factor Va–Xa, has been shown to be dependent on the size of the phospholipid surface surrounding the enzyme (Giesen et al., 1991a). Our experiments with annexin V showed little inhibition at high TF densities and more inhibition at lower densities, which thus agrees with this concept. It also indicates that lateral transport of factor X is not as important for the activity of TF–VIIa as it is for prothrombinase complex activity (Andree et al., 1992).

The technique we used for determining the Xa occupancy of the wall enabled us to determine an equilibrium binding constant for the association of human factor Xa and PS/PC: 33 nM. This, in turn, allowed a computation of the concentration of Xa in the product boundary layer in proximity to the surface: Xa occupied 75% of the available sites. With a K_d of 33 nM, this implies that the product concentration in the vicinity of the wall was of the order of 100 nM. The reason the product concentration is so high near the wall is that product accumulates in a boundary layer that is opposite in gradient from that observed with substrate. Thus, product concentration is highest in the vicinity of the wall and lowest in the mainstream. This follows from the inherent symmetry of the reactive tube; the flux to the wall and flux from the wall can be described with the same equations (Kobayashi & Laidler, 1974; Cussler, 1984, p 300).

Thus, we may construct a model of the local environment in which the TF–VIIa complex functions: The phospholipid is mainly occupied with Xa. Further, the local substrate concentration is minimal (at the transport rate limit), and the concentration of product vastly exceeds that of substrate (see Figure 7). We may conclude from these observations that product inhibition is negligible.

We speculate that the Xa concentrations in which catalysis occurs lends credence to the view that Xa may accelerate the activation of factor IX, an alternate substrate, by TF–VIIa. This was first suggested by Kalousek et al. (1975), who demonstrated that Xa could, in fact, activate factor IX, and was further investigated by Lawson and Mann (1991), who showed that Xa preferentially cleaved an Arg^{145}–Ala^{146} bond which is a slow step in the activation of factor IX catalyzed by TF–VIIa. The data we present here, however, indicate that factors VIII and IX will contribute to factor X activation only under conditions in which the activation of factor X by TF–VIIa is kinetically controlled; that is, limited by the amount of TF–VIIa available for catalysis.

Finally, we wish to point out two salient features of the system described in this paper: (1) At equivalent enzyme densities the concentration of substrate at the wall is much higher when PC is the supporting phospholipid than in the presence of PS/PC membranes. Inasmuch as collisions with the catalytic complex are linear with substrate concentration, the acceleratory effect of PS/PC cannot be ascribed to the latter increasing local substrate concentrations. Rather, it seems likely that PS/PC directly affects the catalytic efficiency of the enzymatic complex or, by virtue of binding, increasing the efficiency of the substrate. In this regard, it is important to note that hydrodynamic theory predicts that the flow conditions we used will not increase the collision frequency at the wall by virtue of convective flow at the surface. Utilizing the Péclet number, which yields the ratio of convection to Brownian motion (Cussler, 1984, p 227), we have calculated that, at 20 nm from the wall, the contribution of flow to molecular motion, a controlling parameter in collision frequency, is only 0.007. (2) When macroscopic surfaces such as cell surfaces are used as a source of enzyme, if the experimental conditions are such that the reaction is transport rate limited, increasing the enzyme concentrations will not lead to an increase in reaction velocity. Thus, care must be taken when concluding that some TF molecules on cell surfaces are "silent" [see, for example, Le et al., 1992)].

In summary, we have utilized a microcapillary continuous flow enzyme reactor to investigate the behavior of TF–VIIa in activation of factor X. We show, in marked contrast to three-dimensional catalysis, that the system can be half-saturated with very low amounts of enzyme. The value required for half-saturation varies with substrate delivery to the surface: the higher the transport rate, the more enzyme is required to reach half-maximal reaction rates. In effect, this means that the usual Michaelis–Menton parameters cannot be applied to macroscopic surfaces unless the transport rate of substrate to the surface is considered. Thus, while the usual techniques utilizing phospholipid vesicles of diameters of 30–150 nm are convenient for determining intrinsic enzyme parameters, their results cannot be easily extrapolated to describe the situation on cell surfaces where blood coagulation occurs in a (patho-) physiological setting.

ACKNOWLEDGMENT

We thank Dr. A. Guha for providing purified factor X and annexin V. Furthermore, we thank Dr. A. Guha, Dr. J. B. A. Ross, Dr. L. Ye, and Dr. W. Konigsberg for helpful suggestions.

REFERENCES

Andree, H. A. M., Reutelingsperger, C. P. M., Hauptmann, R., Hemker, H. C., Hermens, W. Th., & Willems, G. M. (1990) *J. Biol. Chem. 265*, 4923–4928.

Andree, H. A. M., Stuart, M. C. A., Hermens, W. Th., Reutelingsperger, C. P. M., Hemker, H. C., Frederik, P. M., & Willems, G. M. (1992) *J. Biol. Chem. 267*, 17907–17912.

Bach, R., & Rifkin, D. B. (1990) *Proc. Natl. Acad. Sci. U.S.A. 87*, 6995–6999.

Bach, R., Gentry, R., & Nemerson, Y. (1986) *Biochemistry 25*, 4007–4020.

Berg, H. C. (1983) *Random Walks in Biology*, p 36, Princeton University Press, Princeton, NJ.

Bird, R. B., Stewart, W. E., & Lightfoot, E. N. (1960) *Transport Phenomena*, pp 46, 296, 363, 513–515, John Wiley & Sons, Inc., New York.

Contino, P., Repke, D., & Nemerson, Y. (1991) *Thromb. Haemostasis 66*, 138–140.

Cussler, E. L. (1984) *Diffusion: Mass Transfer in Fluid Systems*, pp 227, 301, Cambridge University Press, New York.

Funakoshi, T., Heimark, R. L., Hendrickson, L. E., McMullen, B. A., & Fujikawa, K. (1987) *Biochemistry 26*, 5572–5578.

Gemmell, C. H., Turitto, V. T., & Nemerson, Y. (1988) *Blood 72*, 1404–1406.

Gemmell, C. H., Nemerson, Y., & Turitto, V. (1990) *Microvasc. Res. 40*, 327–340.

Giesen, P. L. A. (1992) *Production of Thrombin at Macroscopic Surfaces*, Thesis, University of Limburg, Maastricht, The Netherlands, ISBN 90-9004944-4.

Giesen, P. L. A., Willems, G. M., & Hermens, W. Th. (1991a) *J. Biol. Chem. 266*, 1379–1382.

Giesen, P. L. A., Willems, G. M., Hemker, H. C., & Hermens, W. Th. (1991b) *J. Biol. Chem. 266*, 18720–18725.

Gramzinski, R. A., Broze, G. J., & Carson, S. D. (1989) *Blood 73*, 983–989.

Hodgman, C. D. (1961) *CRC Standard Mathematical Tables*, p 316, Chemical Rubber Publishing Co., Cleveland, OH.

Kalousek, F., Konigsberg, W., & Nemerson, Y. (1975) *FEBS Lett. 50*, 382–385.

Kobayashi, T., & Laidler, K. J. (1974) *Biotechnol. Bioeng. 16*, 99–118.

Kop, J. M. M., Cuypers, P. A., Lindhout, T., Hemker, H. C., & Hermens, W. Th. (1984) *J. Biol. Chem. 259*, 13993–13998.

Krishnaswamy, S., Jones, K. C., & Mann, K. G. (1988) *J. Biol. Chem. 263*, 3823–3834.

Lawson, J. H., & Mann, K. G. (1991) *J. Biol. Chem. 266*, 11317–11327.

Le, D. T., Rapaport, S. I., & Rao, L. V. M. (1992) *J. Biol. Chem. 267*, 15447–15454.

Lim, T. K., Bloomfield, V. A., & Nelsestuen, G. L. (1977) *Biochemistry 16*, 4177–4181.

Miletich, J. P., Broze, G. J., & Majerus, P. W. (1981) *Methods Enzymol. 80*, 221–228.

Nelsestuen, G. L., & Broderius, M. (1977) *Biochemistry 16*, 4172–4177.

Nemerson, Y., & Gentry, R. (1986) *Biochemistry 25*, 4020–4033.

Ravanat, C., Archipoff, G., Beretz, A., Freund, G., Cazenave, J.-P., & Freyssinet, J.-M. (1992) *Biochem. J. 282*, 7–13.

Repke, D., Gemmell, C. H., Guha, A., Turitto, V. T., Broze, G. J., & Nemerson, Y (1990) *Proc. Natl. Acad. Sci. U.S.A. 87*, 7623–7627.

Reutelingsperger, C. P. M., Kop, J. M. M., Hornstra, G., & Hemker, H. C. (1988) *Eur. J. Biochem. 173*, 171–178.

Schoen, P., Lindhout, T., Willems, G., & Hemker, H. C. (1990) *Thromb. Haemostasis 64*, 542–547.

Tait, J. F., Gibson, D., & Fujikawa, K. (1989) *J. Biol. Chem. 264*, 7944–7949.

Thiagarajan, P., & Tait, J. F. (1990) *J. Biol. Chem. 265*, 17420–17423.

Waxman, E., Laws, W. R., Laue, T. M., Nemerson, Y., & Ross, J. B. A. (1993) *Biochemistry 32*, 3005–3012.